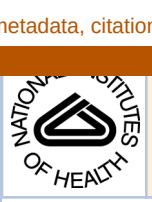

Published in final edited form as:

J Am Chem Soc. 2011 July 13; 133(27): 10368–10371. doi:10.1021/ja2036628.

Enhancing Protease Activity Assay in Droplet-Based Microfluidics Using a Biomolecule Concentrator

Chia-Hung Chen[+,‡], **Aniruddh Sarkar**[+], **Yong-Ak Song**[+,‡], **Miles A. Miller**[‡], **Sung Jae Kim**[+,‡], **Linda G. Griffith**[‡], **Douglas A. Lauffenburger**[‡], and **Jongyoon Han**[+,‡,*]

[+]Department of Electrical Engineering and Computer Science, MIT, 36-841, 77 Massachusetts Avenue, Cambridge MA 02139

[‡]Department of Biological Engineering, MIT, 56-651, 77 Massachusetts Avenue, Cambridge MA 02139

Abstract

We introduce an integrated microfluidic device consisting of a biomolecule concentrator and a microdroplet generator, which enhances the limited sensitivity of low-abundance enzyme assays by concentrating biomolecules before encapsulating them into droplet microreactors. We used this platform to detect ultra low levels of matrix metalloproteinases (MMPs) from diluted cellular supernatant and showed that it significantly (~10-fold) reduced the time required to complete the assay and the sample volume used.

Keywords

protease; biosensors; microemulsion; analytical methods

Secreted active proteases, from families of enzymes such as matrix metalloproteinases (MMPs), participate in diverse biological and pathological processes[1]. As the key degradative enzymes of the extracellular matrix, MMPs play a critical role in cancer development and metastasis[2]. However, the activity of these enzymes has been difficult to measure because of their low abundance, and correspondingly long reaction times necessary to turn over sufficient substrate for detection[3-5]. Existing enzyme activity assays either lack the sensitivity required to directly detect the protease activity in limited sample quantities[6-8] or suffer from low throughput[9-11].

Droplet-based microfluidics has been widely applied to improve many analytical methods in chemistry and biology[12], such as high-throughput screening[13-15], protein crystallization[16,17], cell encapsulation[18,19] and enzymatic assays[20,21]. The ability to run massively parallel reactions in thousands of droplets is desirable in order to monitor the enzymatic activity of physiological samples using extremely small amounts of sample and reagents[12,13,15]. However, the analysis of low-abundance enzymes directly from physiological samples in droplets is challenging because of the low assay sensitivity, the long assay times and the nonspecific loss of target biomolecules to droplet interfaces. Random encapsulation of individual biomolecules into droplets could increase the effective concentration within droplets and enhance the assay sensitivity[18,20-24]. However, this mode of enhancement is limited because even in the smallest stable droplets (diameter ~5 μm), a

jyhan@mit.edu, Tel: (+1) 617-253-2290, Fax: (+1) 617-253-5843.

Supporting Information Available: Detailed experimental procedures, analytical characterization, calibration, β-Gal experiments, kinase experiments and cellular supernatant culture experiments are included in the supporting information.

single trapped molecule is equivalent to an effective concentration of ~1pM, which is below the detection limit of many conventional assays, such as capillary electrophoresis-based assays[25] and immunoassays[26]. So far, methods for controlling reactant concentrations in droplets[12,27-32] rely on further dilution of the sample to tune the ratio of the different reactants. Thus, a reliable and programmable method to increase the concentration of biomolecules within droplets is required to take advantage of the full potential of droplet-based microfluidics.

Previously, a nanofluidic biomolecule concentrator based on ion concentration polarization phenomenon[33] has been developed for trapping and collecting proteins in a sample into a pL-scale plug. This concentrator exhibits local concentration enhancement up to a millionfold. This technique has been employed to increase the sensitivity of protein immunoassays[34], enzyme activity assays[11] and kinase assays using unfractionated cell lysates[9] without changing the biochemistry involved (e.g., the quality of antibody) in the assay. However, the localized high concentration sample plug can easily disperse during downstream processing and observation[35]. Thus, the reactions in these concentration-enhanced assays are usually run in continuously accumulating plugs[36] (non-equilibrium reaction), which complicates the interpretation of the results.

Here, we have integrated a biomolecule concentrator and a droplet generator in a single chip, exploiting the complementary advantages—sensitivity enhancement and effective encapsulation—of these two technologies. Additionally, the multiplexed assays can be completed with a minimal amount of sample reagent because numerous droplets that have different sample concentrations are used as individual reaction chambers. Thus, this integrated device has the ability to detect low-abundance enzymes and other relevant biomarkers in complex physiological samples with high sensitivity and throughput, and therefore can be a generic tool for systems biology research and medical diagnostics. We used this platform to analyze protease MMP activity directly from cellular supernatants and demonstrated a significant (~10-fold) increase in the reaction rate and a consequent reduction in the reaction time. We used less than 25μL of diluted cellular supernatant to simultaneously probe up to 10 different reaction conditions, a task that would have been extremely difficult using existing analytical methods.

The device shown in the schematic diagram (Figure 1A) was fabricated (details in S1) as a Polydimethylsiloxane (PDMS) chip bonded to a PDMS-coated glass slide. We introduced three aqueous streams into the device using syringe pumps (Harvard, PHD2000). The sample in the middle channel contained the target enzyme and a fluorescent tracer (Alexa Fluor-546 phalloidin, λ_{ex}=561nm; λ_{em}=572nm). The two side channels contained the substrate for the enzyme activity assays, to be mixed just before droplet formation. The biomolecule concentrator consisted of polymeric nanoporous (ion-selective) junctions between the microchannels, and a voltage could be applied using buffer channels on either side across the planar ion-selective membrane. To concentrate the biomolecules, we applied a voltage across the main channel (containing the sample) and the side channels (containing buffer solution) to produce an electrokinetically driven force in the main channel[37-40], which pushed negatively charged molecules in the opposite direction of the flow.

The sample flow rate (0.03μL/min) and the applied voltage (~50V) were adjusted so that the electrokinetic force balanced the pressure-driven flow to trap the biomolecules at the boundary and continuously accumulate them into a plug. This plug was monitored by the fluorescence (λ_{ex}=561nm; λ_{em}=572nm) of the added tracer, as shown in Figure 1B. The enhancement factor of the biomolecule concentration in the plug could be varied by choosing the concentration time and was tuned to be ~100-fold. After sufficient accumulation, the plug was released by turning off the voltage, was transported by pressure-

driven flow and was mixed with the substrate coming in from the side channels in the mixing zone (Figure 1C). The mixing ratio of enzyme and substrate was controlled by adjusting the flow rates of three aqueous streams to ensure a ratio of 1:1 between the enzyme (sample) and substrate solutions. The plug containing the assay mixture was then sent to the droplet generator for encapsulation (details in S2, see supporting video) and the maximum concentration enhancement reduced to ~20-fold at this stage due to dispersion during transport and mixing.

A flow-focusing geometry was used as the droplet generator with fluorocarbon oil as the carrier fluid (Figure 1D). The hydrophobic PDMS surfaces in the device caused the aqueous solution containing the enzyme-substrate mixtures to lift off and become encapsulated in the oil, forming a monodisperse water-in-oil emulsion. The oil flow rate was kept at 1.0 μL/min to match the aqueous flow rates used to form the droplets (~40pL volume with a generation rate of ~2.5kHz). Because the volume of the reaction mixture plug was larger than the droplet size, the plug was divided into several droplets with different enhanced enzyme concentrations with a constant substrate concentration (Figure 1F). The enzyme and substrate spontaneously mixed well as the result of the vortices induced inside the droplets[41] which were stabilized by dispersing a synthesized biocompatible surfactant (details in S3) [12,42,43] in the oil phase ensuring that the contents remained isolated for individual reactions. All droplets were monitored using the tracer fluorescence and reaction product fluorescence (Figure 1E, details in S4). This scheme enabled the simultaneous observation of the activities at different enzyme concentrations, resulting in a high assay throughput.

To characterize the microfluidic platform, we detected and the activity of the β-galactosidase (details in S5) and the kinase MK2 (details in S6). After these tests, we employed this platform to study the activity of a recombinant matrix metalloproteinase (MMP-9, 0.2nM) in MMP buffer using a FRET-based polypeptide MMP substrate (5μM), which fluoresces upon cleavage as an indicator of proteolytic activity. MMP-9 activity was monitored in the individual droplets. We observed very small fluorescence changes (~25a.u.) for the negative-control samples lacking protease (Figure 2A). For droplets containing the protease, the fluorescence intensities of the turned-over substrate increased linearly with assay time in both experiments with and without the concentration step. After the preconcentration step, the concentration of MMP-9 in the droplets increased up to 16-fold (inferred by the tracer fluorescence) which correlated with the identical increase in activity measured using product fluorescence.

Additionally, different enzyme concentrations (from 0.2nM to 3.2nM) were screened in a single experiment to obtain information on reaction kinetics, as shown in Figure 2B. The concentration range could be tuned by selecting the distance. As expected, the reaction rates showed an almost linear increase with increasing MMP-9 concentration. After calibration of the fluorescence intensity of the product (details in S7), the value of the kinetic constant ($k_{cat}/K_m = 7.81*10^4\ M^{-1}\ S^{-1}$) was obtained by assuming that Michaelis-Menten kinetics were obeyed. This result was consistent with the value obtained using a standard plate-reader (details in S8) and with the value from a previous study on protease activity[2].

We then performed the experiments with diluted conditioned media from in vitro tissue culture samples (0.5× cellular supernatant dilutions in MMP buffer) to study the protease activity in the media. Specifically, we examined stimulated and untreated protease activity of the culture media from mouse embryonic fibroblasts (MEF) in response to cytokine treatment. The details of the cell culture are described further in the supporting information (details in S9). For both stimulated and untreated samples, the proteolysis reaction caused the fluorescence intensity to increase linearly over time (Figure 3A). After concentrating the

sample, the difference in activity between the stimulated and untreated samples was amplified ~10-fold compared to difference between the unconcentrated samples. The detection sensitivity for the stimulated and untreated conditions was thus improved, allowing us to clearly differentiate these conditions by the slopes of the fluorescence intensity increase over 5 min (line-1 slope: 2.14a.u./s, line-3 slope: 0.95a.u./s). In the unconcentrated assay, the traces of the stimulated condition (line-2 slope: 0.32a.u./s) were significantly different from those of the untreated condition (line-4 slope: 0.22a.u./s) only after 50 min of reaction time. Taking advantage of the high-throughput screening made possible by using our device (Figure 3B), the reaction rates over a range of concentration enhancements were determined by a single experimental run to obtain the parameters related to the reaction kinetics (stimulated sample: $(k_{cat}/K_M)[E] = 1.61*10^{-4}S^{-1}$; untreated sample: $(k_{cat}/K_M)[E] = 4.68*10^{-5}S^{-1}$). This experiment required less than 25μL of diluted cellular supernatant. This is a ~100-fold reduction in sample volume compared to conventional assays. More details are shown in the supporting information (details in S10).

In summary, we developed a microfluidic platform that integrates a biomolecule concentrator and a droplet generator to detect enzyme activity with high sensitivity in a high-throughput manner. This system can be used to analyze different enzyme reactions, such as those catalyzed by reporter enzymes, kinases and proteases. We specifically characterized the activity of MMPs in diluted cellular supernatant from stimulated and untreated MEF cells. The concentrator amplified the difference between the stimulated and untreated conditions and allowed a significant reduction in the reaction time (~10-fold). Moreover, the protease-substrate reaction kinetics could be determined by a parallel analysis of droplets with different amplified enzyme concentrations in a single experiment to significantly reduce the sample volume used (~100-fold). This device, with its ability to assay biochemical reactions catalyzed by low-abundance enzymes and other relevant biomarkers in physiologically complex samples, is a generic and useful platform for systems biology research and medical diagnostics.

Supplementary Material

Refer to Web version on PubMed Central for supplementary material.

Acknowledgments

We gratefully acknowledge Dr. R. Sperling for help with the surfactant synthesis and the financial support of this research by the NIH GM68762, U54-CA112967, R01-EB010246, R01-GM081336, NSF Graduate Fellowship to M.A.M. and DARPA Cipher Program.

References

1. Wolf K, Wu YI, Liu Y, Geiger J, Tam E, Overall C, Sharon M, Friedl P. Nat Cell Biol. 2007; 9:893. [PubMed: 17618273]
2. Miller MA, Barkal L, Jeng K, Moss M, Herrlich A, Griffith L, Lauffenburger D. Inter Biol. 2011; 3:422.
3. Kleiner D, Stetler-Stevenson W. Anal Biochem. 1994; 218:325. [PubMed: 8074288]
4. Oliver G, Leferson J, Stetler-Stevenson W, Kleiner D. Anal Biochem. 1997; 244:161. [PubMed: 9025922]
5. Hughes AJ, Herr AE. Anal Chem. 2010; 82:3803. [PubMed: 20353191]
6. J N, Saghatelian Alan, Joseph Arul, Humphrey Mark, Cravatt Benjamin F. Proc Natl Acad Sci USA. 2004:13756. [PubMed: 15356343]
7. M SR, Blum Galia, Keren Kinneret, Fonovic Marko, Jedeszko Christopher, Rice Mark J, Sloane Bonnie F, Bogyo Matthew. Nat Chem Biol. 2005; 1:203. [PubMed: 16408036]
8. Z Y, Yao Hequan, Xiao Fei, Xia Zuyong, Rao Jianghong. Angew Chem In Ed. 2007; 46:3.

9. Lee JH, Cosgrove BD, Lauffenburger DA, Han J. J Am Chem Soc. 2009; 131:10340. [PubMed: 19722608]
10. Lee JH, Song YA, Han J. Lab Chip. 2008; 8:596. [PubMed: 18369515]
11. Lee JH, Song YA, Tannenbaum SR, Han J. Anal Chem. 2008; 80:3198. [PubMed: 18358012]
12. Theberge AB, Courtois F, Schaerli Y, Fischlechner M, Abell C, Hollfelder F, Huck WTS. Angew Chem In Ed. 2010; 49:5486.
13. Agresti JJ, Antipov E, Abate AR, Ahn K, Rowat AC, Baret JC, Marquez M, Klibanov AM, Griffiths AD, Weitz DA. Proc Natl Acad Sci USA. 2010; 107:4004. [PubMed: 20142500]
14. Abate AR, Hung T, Mary P, Agresti JJ, Weitz DA. Proc Natl Acad Sci USA. 2010; 107:19163. [PubMed: 20962271]
15. Brouzes E, Medkova M, Savenelli N, Marran D, Twardowski M, Hutchison JB, Rothberg JM, Link DR, Perrimon N, Samuels ML. Proc Natl Acad Sci USA. 2009; 106:14195. [PubMed: 19617544]
16. Li L, Mustafi D, Fu Q, Tereshko V, Chen DL, Tice JD, Ismagilov RF. Proc Natl Acad Sci USA. 2006; 103:19243. [PubMed: 17159147]
17. Li L, Nachtergaele S, Seddon AM, Tereshko V, Ponomarenko N, Ismagilov RF. J Am Chem Soc. 2008; 130:14324. [PubMed: 18831551]
18. Koster S, Angile FE, Duan H, Agresti JJ, Wintner A, Schmitz C, Rowat AC, Merten CA, Pisignano D, Griffiths AD, Weitz DA. Lab Chip. 2008; 8:1110. [PubMed: 18584086]
19. Huebner A, Srisa-Art M, Holt D, Abell C, Hollfelder F, deMello AJ, Edel JB. Chem Comm. 2007; 12:1218. [PubMed: 17356761]
20. Joensson HN, Samuels ML, Brouzes ER, Medkova M, Uhlen M, Link DR, Andersson-Svahn H. Angew Chem In Ed. 2009; 48:2518.
21. Huebner A, Olguin LF, Bratton D, Whyte G, Huck WTS, Mello AJd, Edel JB, Abell C, Hollfelder F. Anal Chem. 2008; 80:3890. [PubMed: 18399662]
22. Edgar JS, Milne G, Zhao Y, Pabbati CP, Lim DSW, Chiu DT. Angew Chem In Ed. 2009; 48:2719.
23. Derda R, Tang SKY, Whitesides GM. Angew Chem In Ed. 2010; 49:5301.
24. Vincent ME, Liu W, Haney EB, Ismagilov RF. Chem Soc Rev. 2010; 39:974. [PubMed: 20179819]
25. Breadmore MC. Electrophophoresis. 2007; 28:254.
26. Wild, D. The immunoassay handbook. 3rd. Vol. Ch.11. 2005.
27. L CA, Bui Minh-Phuong Ngoc, Han KN, Choo J, Lee K, Seong GH. Anal Chem. 2011; 83:3358. [PubMed: 21456571]
28. Li L, Ismagilov RF. Annu Rev Biophys. 2010; 39:139. [PubMed: 20192773]
29. Dittrich PS, Jahnz M, Schwille P. ChemBioChem. 2005; 6:811. [PubMed: 15827950]
30. Kreutz JE, Li L, Roach S, Hatakeyama T, Ismagilov RF. J Am Chem Soc. 2009; 131:6042. [PubMed: 19354215]
31. Li L, Boedicker JQ, Ismagilov RF. Anal Chem. 2007; 79:2756. [PubMed: 17338503]
32. W G, Theberge Ashleigh B, Huck Wilhelm TS. Anal Chem. 2010; 82:3349.
33. Wang YC, Stevens AL, Han J. Anal Chem. 2005; 77:4293. [PubMed: 16013838]
34. Wang YC, Han J. Lab Chip. 2008; 8:392. [PubMed: 18305855]
35. Kim SJ, Li L, Han J. Langmuir. 2009; 25:7759. [PubMed: 19358584]
36. Sarkar A, Han J. Lab Chip. 2011 10.1039C0LC00588F.
37. Kim SJ, Wang YC, Lee JH, Jang H, Han J. Phys Rev Lett. 2007; 99:044501. [PubMed: 17678369]
38. Kim P, Kim SJ, Suh KY, Han J. Nano Lett. 2010; 10:16. [PubMed: 20017532]
39. Kim SJ, Ko SH, Kang KH, Han J. Nat Nanotechnol. 2010; 5:297. [PubMed: 20305644]
40. Probstein, RF. Physicochemical Hydrodynamics: An Introduction. Wiley-Interscience; 1994.
41. Chen DL, Gerdts CJ, Ismagilov RF. J Am Chem Soc. 2005; 127:9672. [PubMed: 15998056]
42. Holtze C, Rowat AC, Agresti JJ, Hutchison JB, Angile FE, Schmitz CHJ, Koster S, Duan H, Humphry KJ, Scanga RA, Johnson JS, Pisignano D, Weitz DA. Lab Chip. 2008; 8:1632. [PubMed: 18813384]

43. Song H, Chen DL, Ismagilov RF. Angew Chem In Ed. 2006; 45:7336.

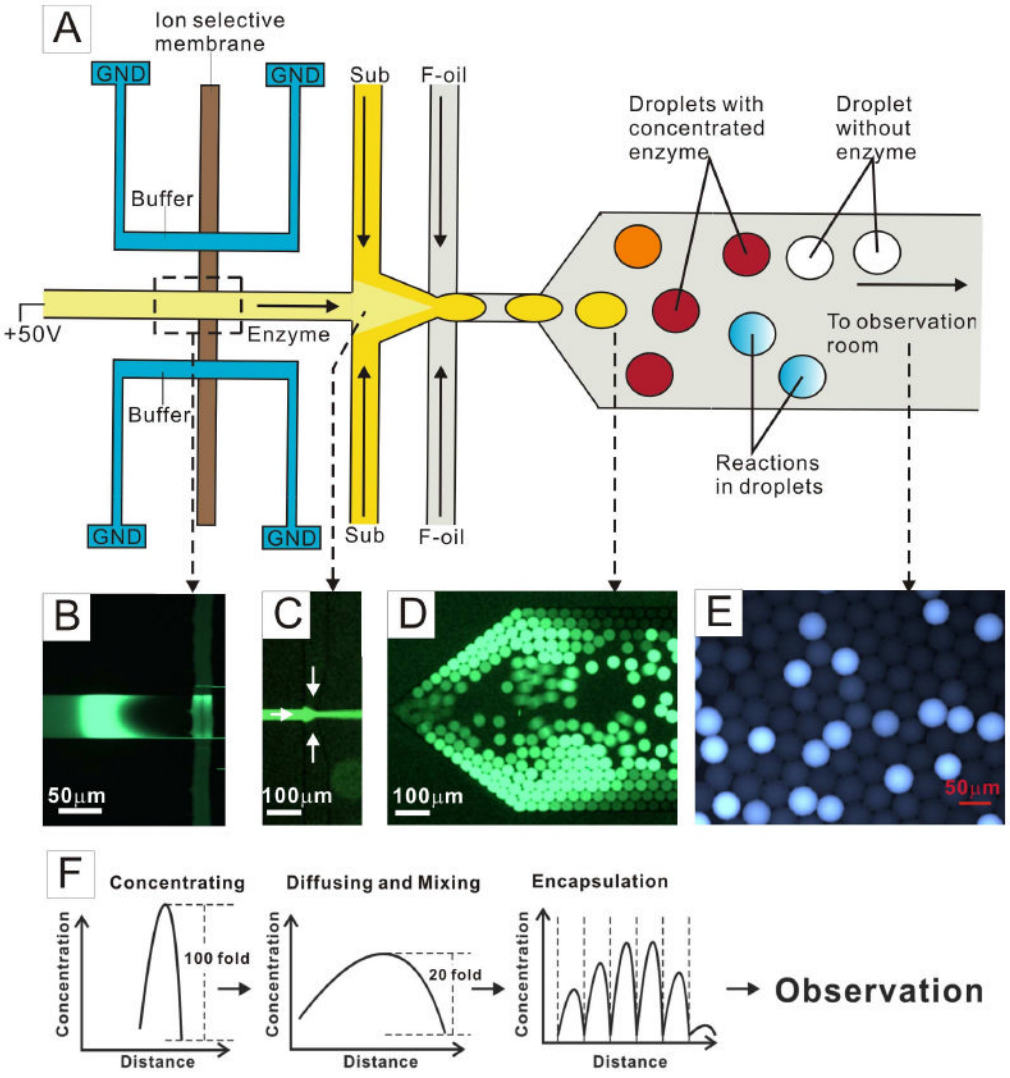

Figure 1.

(A) Schematic representation of the integrated nanofluidic biomolecule concentrator and microfluidic droplet generator chip. (B) The enzyme molecules were accumulated by a concentrator into a plug that (C) was mixed with the substrate and (D) then encapsulated into monodisperse microdroplets for time-dependent observation. (E) The reaction to turn over the fluorogenic substrate was monitored as a function of time in the droplets. (F) The scheme shows that the concentrated plug diffuses as it travels from the concentrator to the point where it is encapsulated in immiscible fluid (~200μm). Then, the plug is divided into several droplets with different enzyme concentrations for parallel screening.

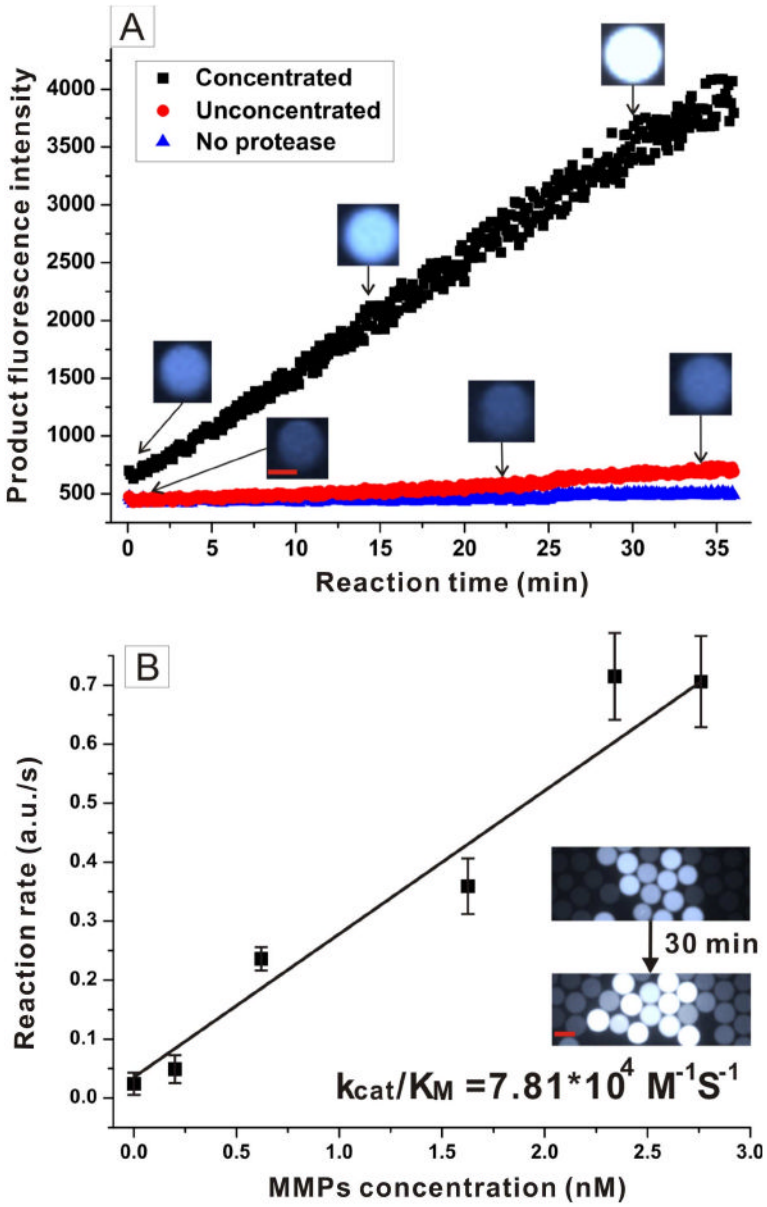

Figure 2.

(A) The product fluorescence intensity increase in each individual droplet with reaction time (after mixing the MMP and the sensor) is shown. The reaction rate exhibited a 15-fold increase because of the enhancement of the recombinant protease MMP-9 concentration. The scale bar in the figure is 25μm. (B) In this plot, the reaction rate increased as the MMP concentration in the droplets increased. The protease concentrations were inferred by comparing the tracer dye intensity to that of the droplet without enzyme (0.2nM). Different concentrations were analyzed in a single experiment to obtain the reaction kinetics constants. Each data point represents the average of five droplets, and the error bar represents the standard deviation. The scale bar in the figure is 50μm.

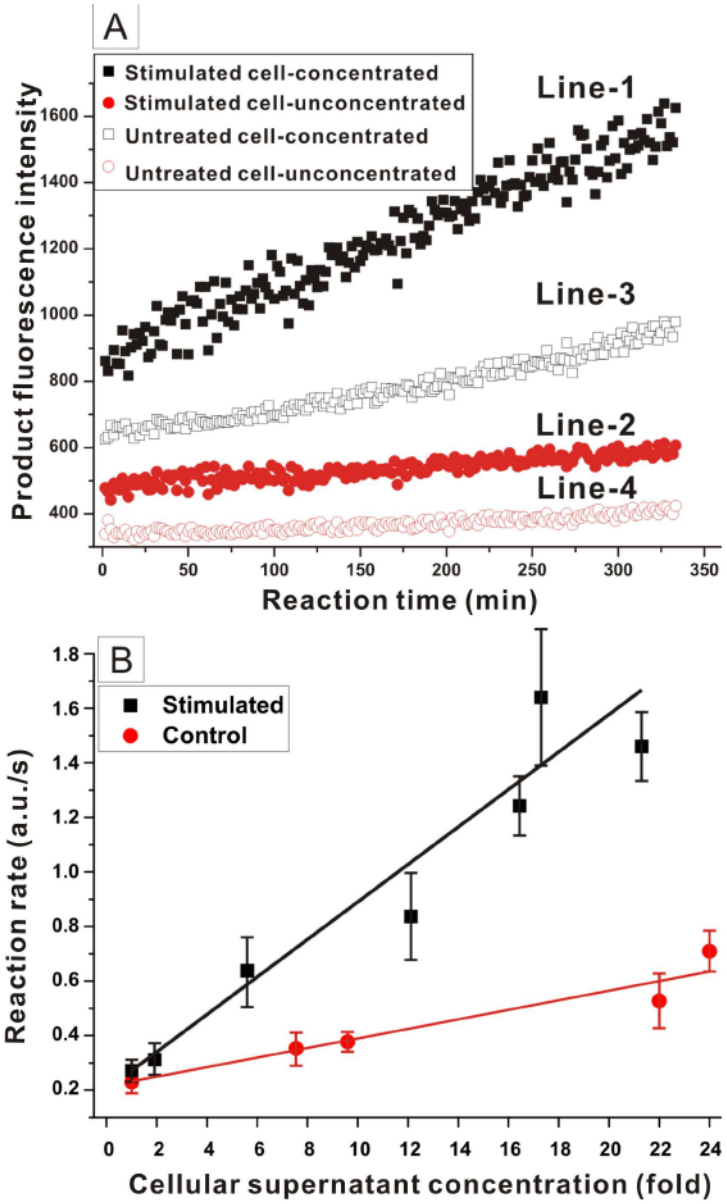

Figure 3.

(A) The increase in the product fluorescence intensity in an individual droplet with reaction time (after mixing the cellular supernatant and the sensor) is shown. The reaction rates, as determined by substrate turnover resulting from proteolysis in cellular supernatant, were monitored as a function of time. The activities of the stimulated samples (concentrated and unconcentrated) are represented by line-1 and line-2, respectively. The activities of untreated samples are shown in line-3 (concentrated) and line-4 (unconcentrated). The difference in the reaction rates was greater for the concentrated samples than for the unconcentrated samples, and thus, the assay sensitivity was improved. (B) The reaction rate increased with increasing cellular supernatant concentrations in the droplets. A linear relation was observed between the reaction rate and the initial concentration. Each data point represents the average of five droplets, and the error bar represents the standard deviation.